Determination of Cluster Hydrodynamics in Bubbling Fluidized Beds by the EMMS Approach

Farzaneh Moradgholi, Navid Mostoufi * and Rahmat Sotudeh-Gharebagh
Oil and Gas Processing Centre of Excellence, School of Chemical Engineering, College of Engineering, University of Tehran, Tehran, Iran
(Received 2 October 2011, Accepted 14 December 2011)

Abstract

The local solid flow structure of gas-solid bubbling fluidized bed was investigated to identify and characterize the particle clusters. Extensive mathematical calculations were carried out using the energy-minimization multi-scale (EMMS) approach for evaluating cluster properties including the velocity, the size and the void fraction of clusters in the dense phase of the bed. The results showed that by increasing the gas velocity, the void fraction of clusters increases and also the larger portion of solids move in the bed in the form of cluster. Modeled results were in good agreement with the experimental data reported in literature in terms of the velocity, the size the void fraction of clusters. The results of this study help to comprehend the hydrodynamics of clusters in gas-solid bubbling fluidized beds.

Keywords: EMMS, Bubbling fluidized bed, Cluster velocity, Cluster diameter

Introduction

Formation, breakup and reassembly of particle aggregates are common hydrodynamic features in fluidized beds [1]. Many researchers experimentally investigated these phenomena in beds. Li et al. [2], Horio and Kuroki [3] and Lin et al. [4] used optical probes to detect clusters in the riser. Soong et al. [1] detected clusters with capacitance probes. Zhou et al. [5] used a video camera to identify clusters in the riser by micrographs. In order to better understand the nature of clusters, some criteria have been proposed to identify clusters in terms of quantitative characteristics such as time fraction, frequency, duration time, average solids concentration and vertical size of clusters in the riser [1, 6-7]. However, less attention has been paid to clusters in the dense phase of fluidized beds in bubbling and turbulent regimes compared to those in fast fluidization regime due to the complex flow structure of the solids in the dense phase.

Cui et al. [8] provided evidences for existence of clusters in the dense phase of bubbling and turbulent fluidized beds and estimated the cluster diameter from the effective solids velocity in the bed. Mostoufi and Chaouki [9] investigated cluster diameter and cluster velocity at different superficial gas velocities by radioactive particle tracking technique. Afsahi et al. [10] investigated local solid flow structure of bubbling fluidized bed filled with sand particles to characterize clusters using an optical fiber probe. They measured the velocity and the diameter of clusters. Recently, Cocco et al. [11] used high-speed video imaging inside the fluidized bed and found that the dominant mechanism for clusters in the freeboard appears to be cluster formation in the bed. However, limited modeling efforts were made in literature on cluster properties in the dense region of fluidized beds.

Solids in a fuidized bed do not independently move but as aggregates such as bubble wakes, bubble clouds and clusters. Majority of the solid particles do not move individually but form clusters. Each single particle is attached to a solid aggregate in the dense bed and moves with it until the solid aggregate breaks-up. Therefore, knowing the hydrodynamic properties of these clusters (i.e., size, voidage and velocity) is important for providing an accurate estimation of performance of fluidized bed reactors.

Both particle and the fluid phases have their respective movement tendencies. That

* Corresponding author: Tel: +98- 21-66976863 Fax: +98- 21-66461024 Email: mostoufi@ut.ac.ir

is, particles tend to rearrange themselves with minimal potential energy, while the fluid tends to choose an upward path with minimal resistance when interacting with particles, as postulated by Li and Kwauk [12]. Depending on the relative dominance of either of these two tendencies, three broad regimes of operation are possible:

- Particle-dominated (PD): When the fluid cannot induce the movement of particles, as is in the fixed bed, the particles are said to dominate the particle-fluid system.
- Fluid-dominated (FD): When fluid flow acquires sufficient force to move the particles to follow its movement tendency, the fluid is said to dominate the particle-fluid system.
- Particle-fluid-compromising (PFC): When neither the fluid nor the particles can dominate the other in displaying either's tendency exclusively, as is in fluidization they have to compromise each other in such a way that both yield themselves to the other to some extent, leading to the PFC regime [13].

The variational criterion for particle-fluid systems is regime-specific due to its critical dependence on the relative dominance between the fluid and particles. Without considering this regime-dependent nature of the variational criterion, the system stability of gas-solid flow cannot be correctly represented. The energy minimization multi-scale (EMMS) model was originally developed for describing the gas–solid heterogeneous flow system[12] and recently has been validated by discrete pseudo-particle method [14]. The EMMS model, as shown in Figure 1, can explain the fluidization phenomena. In this model, which is used for analyzing gas–solid fluidized beds, the energy of the system, by considering hydrodynamic constraints, is minimized. The multi-scale capability of EMMS and its well-known abilities in energy minimization make it a promising tool to investigate the properties of clusters. Therefore, the main objective of this study is to characterize the hydrodynamic properties of clusters in dense bubbling fluidized beds using the EMMS model by considering the fact that the gas-solid system always operates in a condition which the energy of the system is minimum. The Doubly Stochastic Poisson Process (DSPP) [15], widely used in both social and natural sciences [16], was also adapted to analyze the fluctuations of solid volume fraction in the dense bed.

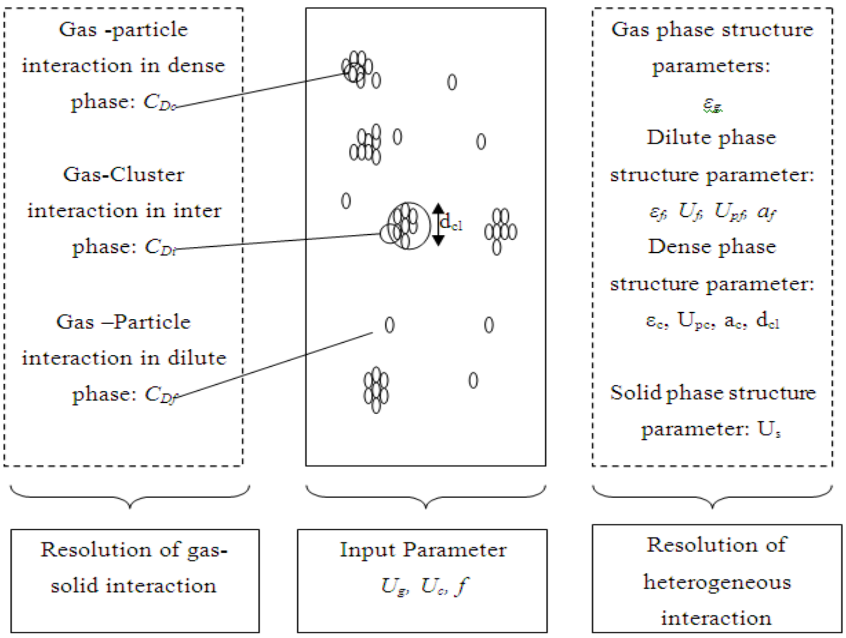

Figure 1: The EMMS approach schematic

Table 1: Comparing parameters of revised EMMS with previous studies

Input (Bubbling)	Output (Bubbling)	Input [12] (Fast fluidization)	Output [12] (Fast fluidization)
U_g	ε_c	U_g	ε_c
U_c	ε_f	U_s	ε_f
F	U_s	ε_g	U_c
d_p	U_f	d_p	U_f
ρ_p	U_{pc}	ρ_p	U_{pc}
ε_{mf}	U_{pf}	ε_{mf}	U_{pf}
U_{mf}	a_c	U_{mf}	a_c
ρ_g	a_f	ρ_g	a_f
μ_g	d_{cl}	μ_g	d_{cl}
μ_p	ε_g	μ_p	f

1. Modeling

In the present study, it was preferred to find the status of the system at minimal energy conditions. The total energy consumption per unit mass of the particles (N_t) comprises of two parts. The first part is the suspending-transporting energy (N_{st}) used for suspending and transporting of the particles and the second part, which is the dissipation energy (N_{dis}), reflects the energy dissipated in collisions, circulations and acceleration of particles and viscous dissipation as well as suspending particles. The EMSS approach tends to minimize the total energy consumed by the system.

In previous studies reported in literature for the riser of fast fluidized-beds, the following EMMS parameters were used [3, 12, 18-20].

$$X=(\varepsilon_f, \varepsilon_c, U_f, U_c, U_{pf}, U_{pc}, f, a_f, a_c, d_{cl}) \qquad (1)$$

However, in the present work, which investigates the hydrodynamics of clusters in bubbling fluidized bed, the following EMMS parameters were considered:

$$X=(\varepsilon_f, \varepsilon_c, U_s, U_f, U_{pf}, U_{pc}, a_f, a_c, d_{cl}) \qquad (2)$$

A comparison among these parameters at different fluidization regimes is done in Table 1. As can be seen in this table, the main difference between the two methods is the way of calculating the void fraction of clusters and velocity of solids. In the present work, the void fraction of cluster and the velocity of solids are calculated by the EMMS method while in the previous works, the velocity of solids is known and cluster velocity and solids fraction is obtained from the EMMS model.

1.1. Assumptions

The following assumptions were considered for estimating the cluster properties by the EMMS approach:

- The flow is uniform and steady within each phase.
- The clusters can have various void fractions as dispersed in a gas–solid mixture.
- Clusters are individual spherical species moving inside the emulsion phase.
- Clusters and particles co-exist simultaneously.

1.2. The EMMS model Formulation

The model was formulated in a nonlinear form with ten variables with the following stability condition [21]:

$$N_{st} = \frac{1}{(1-\varepsilon_g)\rho_s}\left[m_f F_f U_f + m_c F_c U_c + m_i F_i U_f (1-f)\right] \qquad (3)$$

For which N_{st} approaches the minimum. This condition expresses the compromise between the tendency of the fluid to pass through the particle layer with minimum resistance and the tendency of the particle to maintain smallest amount of gravitational potential [13]. The hydrodynamic equations and the corresponding expressions needed for solving the model and for evaluating the diameter of clusters are summarized in Tables 2-4.

Table 2: Summary of hydrodynamic equations for the EMMS model [8]

Description	Formula
Force balance for the clusters in unit volume of suspension	$\left(\frac{3}{4}\right)C_{dc}\frac{f(1-\varepsilon_c)}{d_p}\rho_g U_{sc}^2+\left(\frac{3}{4}\right)C_{di}\frac{f}{d_{cl}}\rho_g U_{si}^2=f(1-\varepsilon_c)(\rho_s-\rho_g)(g+a_c)$
Force balance for the dilute phase in unit volume of suspension	$\left(\frac{3}{4}\right)C_{df}\frac{f(1-\varepsilon_f)}{d_p}\rho_g U_{sf}^2=(1-f)(1-\varepsilon_f)(\rho_s-\rho_g)(g+a_f)$
Pressure drop balance between the clusters and the dilute phase	$C_{df}\frac{(1-\varepsilon_f)}{d_p}\rho_g U_{sf}^2+\frac{f}{1-f}\frac{1}{d_{cl}}C_{di}\rho_g U_{si}^2=C_{dc}\frac{f(1-\varepsilon_c)}{d_p}\rho_g U_{sc}^2$
Mass conservation for the fluid	$U_g=U_f(1-f)+U_c f$
Mass conservation for the particle	$U_s=U_{pf}(1-f)+U_{pc} f$
Definition of mean voidage	$\varepsilon_g=\varepsilon_f(1-f)+\varepsilon_c f$
Acceleration relation	$a_c-a_f=\frac{\langle\varepsilon'_s\varepsilon'_s\rangle(\rho_s-\rho_g)g}{C_{am}(\varepsilon_f-\varepsilon_c)f\left[\rho_s(1-\varepsilon_f)+\rho_g\varepsilon_f\right]}$
Solid concentration inside cluster	$\varepsilon_c=\varepsilon_g-n\sigma_\varepsilon$
Variance of solid concentration fluctuation	$\langle\varepsilon'_s\varepsilon'_s\rangle=\varepsilon_s^2\frac{(1-\varepsilon_s)^4}{1+4\varepsilon_s+4\varepsilon_s^2+4\varepsilon_s^3+\varepsilon_s^4}$
Average solid concentration	$\varepsilon_s=1-\varepsilon_g$
Added mass coefficient for the clusters [33].	$C_{am}=\frac{1}{2}\left(\frac{1+2f}{1-f}\right)$
Standard deviation of solid concentration fluctuation	$\sigma_\varepsilon=\varepsilon_s\sqrt{S(\varepsilon_s,0)}$
Static structure factor	$S(\varepsilon_s,0)=\frac{(1-\varepsilon_s)^4}{1+4\varepsilon_s+4\varepsilon_s^2+4\varepsilon_s^3+\varepsilon_s^4}$

Table 3: Summary of expressions for the EMMS model [14]

Parameter	Dense phase	Dilute phase	Inter phase
Effective drag coefficient	$C_{dc}=C_{d0c}\varepsilon^{-4.65}$	$C_{df}=C_{d0f}\varepsilon^{-4.65}$	$C_{di}=C_{d0i}(1-f)^{-4.65}$
Standard drag coefficient	$C_{d0c}=\frac{24}{Re_c}+\frac{3.6}{Re_c^{0.313}}$	$C_{d0f}=\frac{24}{Re_f}+\frac{3.6}{Re_f^{0.313}}$	$C_{d0i}=\frac{24}{Re_i}+\frac{3.6}{Re_i^{0.313}}$
Characteristic Reynolds number	$Re_c=\frac{\rho_g d_p U_{sc}}{\mu_g}$	$Re_f=\frac{\rho_g d_p U_{sf}}{\mu_g}$	$Re_i=\frac{\rho_g d_{cl} U_{si}}{\mu_g}$
Superficial slip velocity	$U_{sc}=U_c-\frac{\varepsilon_c U_{pc}}{1-\varepsilon_c}$	$U_{sf}=U_f-\frac{\varepsilon_f U_{pf}}{1-\varepsilon_f}$	$U_{sf}=\left(U_f-\frac{\varepsilon_f U_{pf}}{1-\varepsilon_f}\right)(1-f)$
Drag force acting on single particle or cluster	$F_c=C_{dc}\frac{\pi d_p^2}{4}\frac{\rho_g}{2}U_{sc}^2$	$F_f=C_{df}\frac{\pi d_p^2}{4}\frac{\rho_g}{2}U_{sf}^2$	$F_i=C_{di}\frac{\pi d_{cl}^2}{4}\frac{\rho_g}{2}U_{si}^2$
Number of particle or cluster in unit volume	$m_c=\frac{(1-\varepsilon_c)f}{\frac{\pi d_p^2}{6}}$	$m_f=\frac{(1-\varepsilon_c)(1-f)}{\frac{\pi d_p^2}{6}}$	$m_i=\frac{f}{\frac{\pi d_{cl}^2}{6}}$

Table 4: Expression used for evaluating cluster properties

Property	Formula
Density of cluster	$\rho_c = (1-\varepsilon_c)\rho_s + \varepsilon_c\rho_g$
Cluster gas relative velocity	$V_{sl} = \frac{U_c}{\varepsilon_c} - U_{cl}$
Standard drag coef icient [22]	$C_{d,0} = \frac{24}{\mathrm{Re}_{cl,t}}\left(1+0.173\,\mathrm{Re}_{cl,t}^{0.657}\right) + \frac{0.413}{1+16300\,\mathrm{Re}_{cl,t}^{-1.09}}$
Effective drag coef icient [9]	$C_d = \varepsilon_f^{-m} C_{d,0}$ $m = 3.02 Ar^{0.22}\,\mathrm{Re}_{cl,t}^{-0.33}\left(\frac{d_{cl}}{d_p}\right)^{0.4}$
Superficial emulsion gas velocity	$U_c = \frac{U_g - fU_b}{1-f}$
Bubble fraction [8]	$f = 0.534 - 0.534\exp\left(-\frac{U_g - U_{mf}}{0.431}\right)$
Bubble velocity [23]	$U_b = U_g - U_{mf} + 0.71\sqrt{gD_b}$
Bubble diameter [24]	$D_b = 0.21 H^{0.8} U_{exc}^{0.42}\exp\left[-0.25U_{exc}^2 - 0.1U_{exc}\right]$
Emulsion voidage [8]	$\varepsilon_c = \varepsilon_{mf} + 0.2 - 0.59\exp\left(-\frac{U_g - U_{mf}}{0.429}\right)$

Table 5: Input Data considered in this study

d_p (μm)	U_g (m/s)	ρ_g (kg/m^3)	ρ_s (kg/m^3)	Ar	ε_{mf} (-)	H (m)
280	0.052-0.82	1.225	2640	2172	0.42	0.2
490	0.15-1.31	1.225	2640	11600	0.42	0.2

1.3. Estimation of Cluster Properties

Cluster velocity

The cluster velocity can be obtained from the following momentum balance equation on the cluster:

$$\frac{\pi}{8}d_{cl}^2 C_d \rho_g V_{cl,sl}^2 + \frac{\pi}{6}d_{cl}^2\rho_g g - \frac{\pi}{6}d_{cl}^2\rho_{cl} g = 0 \tag{4}$$

Drag coefficient

To calculate the inter-phase momentum exchange coefficient (β), the well-known equation of Ergun [25] was employed for porosities less than 0.35 and the correlation of Wen and Yu [26] for porosities greater than 0.35 [27].

$$\beta = \begin{cases} 0.75 C_d \frac{\varepsilon_g \varepsilon_s \rho_g}{d_p}\left|u_g - u_s\right|\varepsilon_g^{-2.65} H_d & \varepsilon_s \le 0.35 \\ 150\frac{\varepsilon_s^2}{\mu_g d_p^2} + 1.75\frac{\varepsilon_g\varepsilon_s\rho_g}{d_p}\left|u_g - u_s\right| & \varepsilon_s > 0.35 \end{cases} \tag{5}$$

The correction of the revised EMMS model was used by introducing the heterogeneous index:

$$H_d = \frac{F_{d,EMMS}}{F_{d,Wen\&Yu}} \tag{6}$$

In which H_d = 1 for the Wen and Yu correlation. The drag coefficient for an isolated particle was evaluated by the correlation proposed by Mostoufi and Chaouki [9].

The effective drag force predicted by the revised EMMS model is [21]:

$$F_{d,EMMS} = \varepsilon_g\left[f(1-\varepsilon_c)(g+a_c) + (1-f)(1-\varepsilon_f)(g+a_f)\right](\rho_s - \rho_g) \tag{7}$$

The drag force in particulate fluidization was correlated by Wen and Yu [26] as:

$$F_{d,Wen\&Yu} = \frac{3}{4} C_d \frac{\varepsilon_g \varepsilon_s \rho_g}{d_p} \left| u_g - u_s \right| \varepsilon_g^{-2.65} \qquad (8)$$

Cluster fraction

Considering the fact that the solids in the bed are either in form of clusters or single particles, the effective drag force exerted on the solids per unit volume can be expressed by following equation:

$$F_{d,EMMS} = (1-\alpha) F_{d,particle} + \alpha F_{d,cl} \qquad (9)$$

The cluster faction (α) was evaluated from Eq. (9) after solving the EMMS equations.

2. Results and discussion

Hydrodynamic properties of clusters in bubbling fluidized bed were calculated and compared with the experimental data available in literature. In order to cover the full range of the bubbling fluidization, the superficial air velocity was varied from 0.052 to 0.82 m/s for 280 μm sand particles and from 0.15 to 1.31 m/s for 490 μm sand particles. The energy of the system was minimized using the genetic algorithm, with the hydrodynamic equations listed in Table 2 as constraints. The properties of particles used in this study are listed Table 5.

2.1. Cluster size

The heterogeneity in the distribution of particles in bubbling fluidized bed has a significant effect on momentum exchange, heat transfer and mass transfer in the bed. Cluster size is a key parameter that can characterize this heterogeneity and has received considerable attention [28-30]. In the present study, the fluctuations of solid concentration were used to investigate the clustering structure of particles in the dense bed of bubbling fluidization. Usually, the cluster is identified when the local instantaneous solid concentration is greater than the time-mean solid concentration by at least *n* times the standard deviation.

The value of *n* has a significant effect on calculating the cluster size in the revised EMMS model. Larger value of *n* results in a smaller cluster size under the same conditions. Thus, in order to show the influence of this parameter on the calculated cluster size and to choose the best value for it, the calculated cluster diameters for various values of *n* were compared with the experimental data of Afsahi et al. [10] and the results are shown in Figs. 2a-b. These figures show that for *n*=3 the model fits the experimental data very well. Therefore, this value was used throughout the rest of this study.

Figs. 2a-b also demonstrates the effect of gas velocity on the size of clusters. As can be observed in these figures, increasing the gas velocity leads to formation of larger clusters due to its effect on increasing the total drag force exerting on particles. However, increasing the cluster size at the same time reduces the average drag force exerted on each particle.

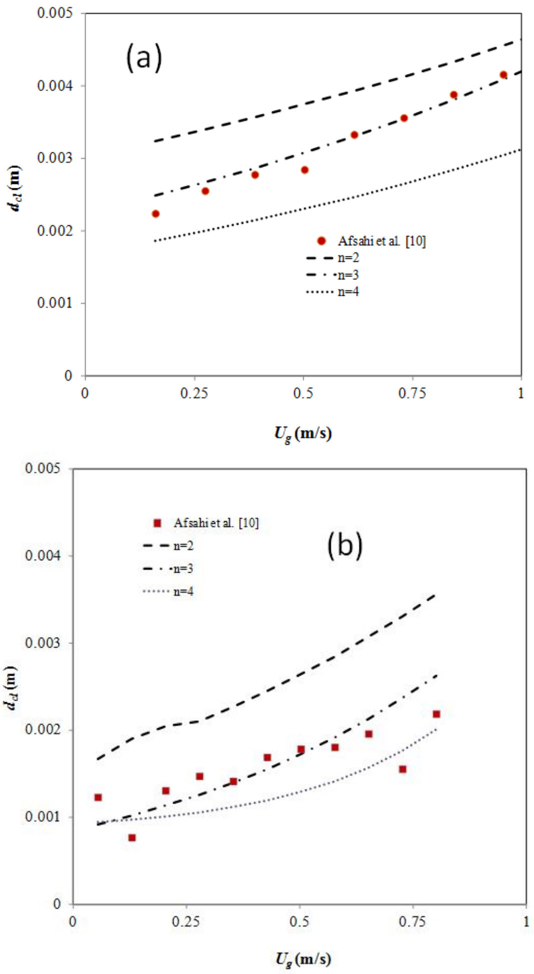

Figure 2: The cluster size from the EMMS model: (a) Effect of solid concentration inside cluster for490 μm particle (b) Effect of solid concentration inside for 280 μm particle

This results in increasing the slip velocity and allows clusters to collect particles and grow in size. Mostoufi and Chaouki [31] reported the same trend for variation of cluster size with gas velocity and obtained the cluster diameter with the same order of magnitude of cluster diameter reported in the present study. It is worth mentioning that at superficial velocities close to the minimum fluidization, calculated cluster size is very close to the size of a particle that indicates clusters do not exist at velocities close to the minimum fluidization.

The cluster size calculated based on the EMMS model was compared with empirical correlations and the results are illustrated in Figs. 3a-b. As shown in these figures, the cluster size increases with an increase in the solids concentration within the clusters. The clusters may maintain a degree of stability against turbulence and collisions because they experience less drag force than individual particles. In addition, reduced drag force increases the slip velocity and allows clusters to collect particles and grow in size. Figs 3a-b also demonstrates that the cluster size estimated by the EMMS model is different from those predicted by the empirical correlations. Such disparity is normal when considering the differences between hydrodynamics of bubbling regime used in this study and that of fast fluidization used for correlations. In fact, previous models shown in Fig. 3a-b were proposed for fully developed section of a circulating fluidized bed riser while the model developed in this work is adopted to the dense bed of a bubbling or turbulent fluidized bed. Therefore, the quantitative agreement with modeling data may not be expected. However, the trends of presented model and the correlations are the same in quite different systems and regimes.

2.2. Cluster velocity

A comparison between the cluster velocities predicted by the EMMS model and the experimental data of Afsahi et al. [10] is shown in Fig. 4. As can be seen in this figure, mean cluster velocity increases with an increase in the superficial gas velocity. This indicates that the fast moving clusters exist at higher gas velocities and a broader range of cluster sizes exist in the bed. Generally, the cluster velocities increase as well with increasing the superficial gas velocity. The reason for such a behavior can be attributed to the fact that when the superficial gas velocity is increased, higher velocities of clusters are achieved by flow of the gas in the bed due to higher momentum transfer between gas and solid. Fig. 4 shows that the experimental data and the numerical results are in fair agreement.

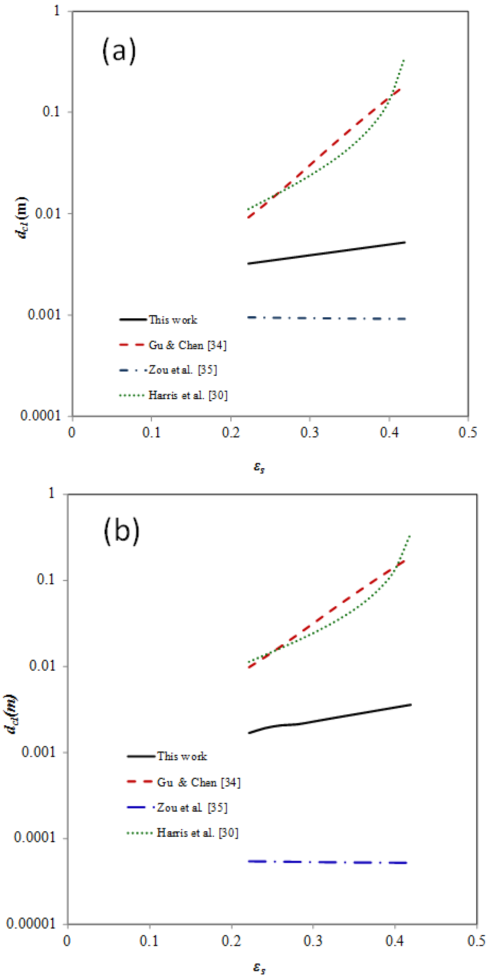

Figure 3: The cluster size from the EMMS model: (a) Comparison with empirically correlated cluster size for 490 µm particle (b) Comparison with empirically correlated cluster size for 280 µm particle

2.3. Cluster fraction

It is possible to evaluate the cluster faction, α, from Eq. (9) by solving the EMMS equations. Fig. 5 illustrates the cluster fraction as a function of superficial gas velocity for two sizes of particles. It can be seen that the cluster fraction increases by increasing the gas velocity. Most of the particles move independently at gas velocities close to the minimum fluidization. However, most of the particles form clusters and grow larger by increasing the gas velocity. Fig. 5 also shows that at high enough gas velocity, the particles move mainly as clusters rather than single particles in the dense bed. This is consistent with the findings of Mostoufi and Chaouki [32] who reported that at low superficial gas velocity, the cluster size is almost equal to the average size of the particles in the bed (i.e., no cluster exists at minimum fluidization). This suggests that the dense phase is mainly in the form of an emulsion of separate particles rather than freely moving clusters while by increasing the gas velocity, the clusters start to form and grow larger. That is, the particles move independently at minimum fluidization condition while by increasing the gas velocity, particle clusters are formed and grow larger since greater drag force can be supplied at higher gas velocity. Fig. 5 also shows that the fraction of particles moving as cluster for smaller particles is higher than that for larger particles at the same gas velocity. This trend indicates that the formation of clusters in a bed of smaller particles occurs easier than in that of larger particles. In fact, the drag force exerted on a single particle per weight of the particle is higher for smaller particles, thus, they tend to form clusters at lower gas velocity in order to reduce the net average drag force exerted on each particle in the cluster.

2.4. Dense phase fraction

Effect of the gas velocity on the dense phase fraction is shown in Fig. 6. As can be seen in this figure, dense phase fraction decreases with increasing the gas velocity due to the increase in the total gas entering the bed. The dense phase fraction obtained by the correlation of Cui et al. [8] is also shown in this figure. As can be seen in Fig. 6, both the EMMS model and the correlation of Cui et al.[8] have the same trend but the EMMS model over-predicts the dense phase fraction. This can be attributed to the different sizes of particles that were used in these two works.

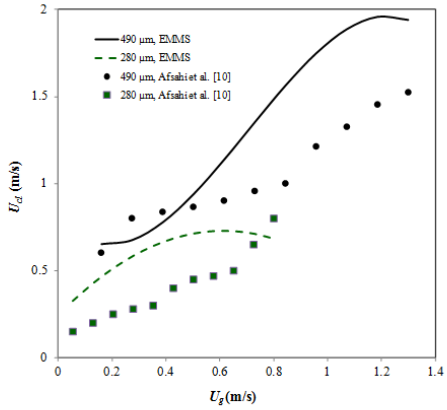

Figure 4: The cluster Velocity from the EMMS model: comparison with empirically correlated cluster size for 490 µm and 280 µm particles

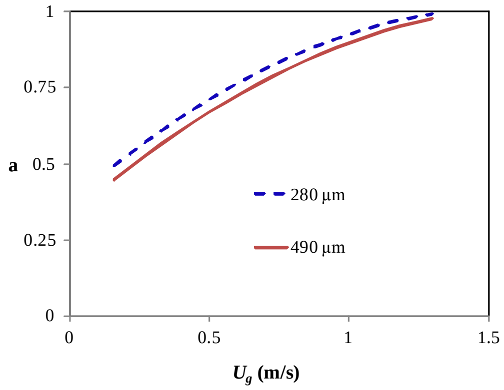

Figure 5: The Cluster Percent at bubbling fluidized bed from the EMMS model for 490 µm and 280 µm particle

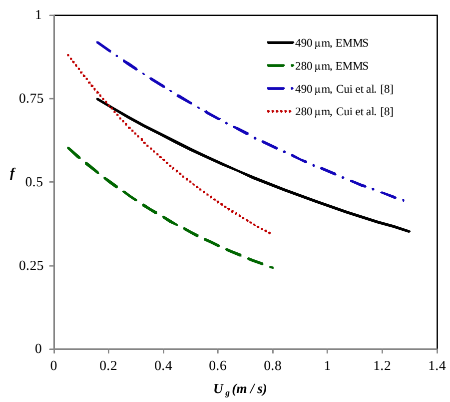

Figure 6: The volume fraction of dense phase from the EMMS model: comparison with empirical correlated for 490 µm and 280 µm particle

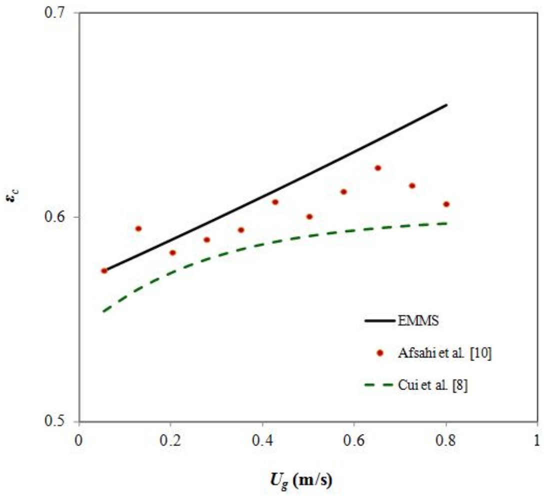

Figure 7: The voidage of dense phase from the EMMS model: comparison with empirical correlated for 490 µm and 280 µm particle

2.5. Void fraction of clusters

Effect of gas velocity on the void fraction of clusters is shown in Fig. 7. This figure shows that increasing the gas velocity results in the formation of clusters with relatively higher void fraction. This means that by increasing the gas velocity higher amount of gas enters into the clusters. Experimental void fraction of clusters reported by Afsahi et al. [10] is also shown in Fig. 7. Comparing the experimental void fraction with those calculated by the EMMS model indicates that there is a reasonable agreement between the values calculated in this work and the experimental ones. The void fraction of emulsion calculated based on the correlation of Cui et al. [8] is also shown in Fig. 7. This figure shows that the clusters are more concentrated in particles than the emulsion.

3. Conclusions

The energy-minimization multi-scale (EMMS) approach was used to investigate the hydrodynamics of bubbling fluidized beds. It was assumed that the solids exist in the bed either as single particles and/or as clusters. Formation of clusters occurs to minimize the energy of the system for modeling of which the EMMS approach was used. The parameters determined by the EMMS model in this study were void fraction of dilute phase, void fraction of clusters, gas velocity, particle velocity and acceleration of particles in the dilute and dense phases as well as the cluster diameter. The abovementioned parameters were determined by minimizing the energy of the system by means of doubly stochastic Poisson processes.

The cluster properties calculated by the EMMS model were found to be in good agreement with the experimental results reported in literature. An important parameter calculated in this work was the fraction of solids that move in the form of clusters in the bed. It was found that most of the particles move independently at low gas velocities. However, particles form clusters and the solid particles mainly exist as clusters at high gas velocities. Void fractions of clusters increased with increasing gas velocity. These values were in fair agreement with the experimental values. The modeling approach proposed in this study allows calculation of cluster properties that can be used to predict the performance of fluidized beds as chemical reactors.

Nomenclature

Ar	Archimedes number $[d_p^3\rho_g(\rho_s-\rho_g)g/\mu_g^2]$
a_c	mean acceleration of particles in dense phase, m/s^2
a_f	mean acceleration of particles in dilute phase, m/s^2
C_D	drag coefficient
C_{Dc}	effective drag coefficient for a particle in dense phase
C_{Df}	effective drag coefficient for a particle in dilute phase
C_{Di}	effective drag coefficient for a cluster
C_{D0}	standard drag coefficient for a particle
d_{cl}	mean cluster diameter, m
d_p	particle diameter, m
f	volume fraction of dense phase
F_d	EMMS drag force, N
F_c	dense phase drag force, N
F_f	dilute phase drag force, N
F_i	inter phase drag force, N
g	gravity of acceleration, m/s^2
g_0	radial distribution function
G_s	solids mass flux, kg/s.m^2
H	bed height, m
H_d	drag force correction factor

M exponent in calculating effective drag coefficient
n experimental fitting factor
N_{st} mass specific energy for suspending and transporting particles, W/kg
Re_{cl} cluster Reynolds number $[d_{cl}\rho_g u_{cl}/\mu_g]$
Re_p particle Reynolds number $[d_p\rho_g u_p/\mu_g]$
Re_t particle terminal Reynolds number $[d_p\rho_g u_t/\mu_g]$
$S(\varepsilon_s,0)$ static structure factor
U_b bubble velocity, m/s
U_c mean superficial fluid velocity in dense phase, m/s
U_{cl} mean cluster velocity, m/s
U_f mean superficial fluid velocity in dilute phase, m/s
U_g superficial gas velocity, m/s
U_{mf} minimum fluidization velocity, m/s
U_{pc} mean superficial particle velocity in dense phase, m/s
U_{pf} mean superficial particle velocity in dilute phase, m/s
U_s mean superficial particle velocity, m/s
U_{sc} mean superficial slip velocity in dense phase, m/s
U_{sf} mean superficial slip velocity in dilute phase, m/s
U_{si} mean superficial slip velocity in inter-phase, m/s
U_t terminal velocity, m/s
X hydrodynamic property

Greek letters

α fraction of solids moving as clusters
β drag coefficient per unit volume, kg/s.m^3
ε_g voidage
ε_s average solid volume fraction
ε_{mf} voidage at minimum fluidization
ε_c voidage of dense phase
ε_f voidage of dilute phase
ε_{sc} solid volume fraction inside cluster,
μ_g gas viscosity, Pa.s
μ_s solid viscosity, Pa.s
ρ_g fluid density, [kg/m^3]
ρ_s solid density, [kg/m^3]
σ_ε standard deviation of solid volume fraction,[-]

Subscripts

e emulsion phase
f bubble phase
g gas phase
mf minimum fluidization
s solid phase
sl slip
t terminal

References:

1- Soong, C. H., Tuzla, K. and Chen, J. C. (1994). Identification of Particle Clusters in Circulating Fluidized Beds, in Circulating Fluidized Beds Technology, A. A. Avidan, Ed., AIChE, New York, 615–620.

2- Li, H., Xia, Y., Tung, Y. and Kwauk, M. (1991). Micro-visualization of cluster in a fast fluidized Bed, Powder Technol., 66 ,231–235.

3- Horio, M. and Kuroki, H. (1994). "Three-dimensional flow visualization of dilute dispersed solids in bubbling and circulating fluidized beds." *Chem. Eng. Sci.*, 49, 2413–2421.

4- Lin, Q., Wei, F. and Jin, Y. (2001). "Transient Density Signal Analysis and Two-Phase Micro Structure Flow in Gas–Solids Fluidization." *Chem. Eng. Sci.*, 56 , 2179–2189.

5- Zhou, B., Li, H., Xia, Y. and Ma, X. (1994). Cluster Structure in a Circulating Fluidized Bed, Powder Technol., 78, 173–178.

6- Sharma, A. K., Tuzla, K., Matsen, J. and Chen, J. C. (2000). Parametric Effects of Particles Size and Gas Velocity on Cluster Characteristics in Fast Fluidized Beds, Powder Technol., 111, 114–122.

7- Manyele, S. V., Parssinen, J. H. and Zhu, J. X. (2002). "Characterizing Particle Aggregates in a High-Density and High-Flux CFB Riser." *Chem. Eng. J.*, 88, 151–161.

8- Cui, H., Mostoufi, N. and Chaouki, J. (2000). "Characterization of Dynamic Gas Solid Distribution in Fluidized Beds." *Chem. Eng. J.*, 79, 135–143.

9- Mostoufi, N. and Chaouki, J. (1999). "Prediction of Effective Drag Coefficient in Fluidized Beds." *Chem. Eng. Sci.*, 54, 851–858.

10- Afsahi, F. A., Sotudeh-Gharebagh, R. and Mostoufi, N. (2009). "Clusters identification and characterization in gas- solid Fluidized bed by the wavelet analysis." *Can. J. Chem. Eng.*, 87, 375-385.

11- Cocco, R., Shaffer, F., Hays, R., Karri, R. and Knowlton, T. (2010). Particle clusters in and above fluidized beds. Powder Technol., 203, 3-11.

12- Li, J. and Kwauk, M. (1994). Particle–Fluid Two-Phase Flow: The Energy- Minimization Multi-Scale Method. Metallurgical Industry Press, Beijing, PR China.

13- Li, J. H., Kwauk, M. and Reh, L. (1992). Role of energy minimization in Gas-solid fluidization. In O. E. Potter and D. J. Nicklin, Fluidization. New York: Engineering Foundation**.** 83-90.

14- Zhang, J. Y., Ge, W. J. and Li, H. (2005). "Simulation of heterogeneous structures and analysis of energy consumption in particle–fluid system with pseudo particle modeling." *Chem. Eng. Sci.*, 60, 3091–3099.

15- Grandell, J. (1976). Doubly Stochastic Poisson Processes. Springer, Berlin, Heidelberg**.**

16- Kostinski, A. B. and Jameson, A. R. (1997). "Fluctuation properties of precipitation. Part 1: on the deviations of single-size drop counts from the Poisson distribution." *J. Atmos. Sci.*, 54, 2174–2186.

17- Lackermeier, U., Rudnick, C., Werther, J., Bredebusch, A. and Burkhardt, H. (2001). Visualization of flow structures inside a circulating fluidized bed by means of laser sheet an image processing. Powder Technol., 114, 71–83.

18- Li, J., Cheng, C., Zhang, Z., Yuan, J., Nemet, A. and Fett, F. N. (1999). "The EMMS model and its application, development and updated concepts." *Chem. Eng. Sci.*, 54, 5409–5425.

19- Cheng, C., Ge, W. and Li, J. (2005). Multi-scale modeling of the axial heterogeneous structure with the EMMS approach. Internal Reports of Institute of Process Engineering, Chinese Academy of Sciences.

20- Wang, W. and Li, J. (2007). "Simulation of gas–solid two-phase flow by a multiscale CFD approach: extension of the EMMS model to the sub-grid scale level." *Chem. Eng. Sci.*, 62, 208–231.

21- Yang, N., Wang, W., Ge, W., Wang, L. and Li, J. (2004). "Simulation of heterogeneous structure in a circulating fluidized bed riser by combining the two-fluid model with the EMMS approach." *Ind. Eng. Chem. Res.***,** 43, 5548–5561.

22- Turton, R. and Levenspiel, O. (1986). A Short Note on the Drag Correlation for Spheres. Powder Technol., 47, 83–86.

23- Davidson, J. F. and Harrison, D. (1963). Fluidized Particles, Cambridge University Press, *Cambridge*.

24- Cai, P., Schiavetti, M., De Michele, G., Grazzini, G. C. and Miccio, M. (1994). Quantitative Estimation of Bubble Size in PFBC. Powder Technol**.,** 80, 99–109.

25- Ergun, S. (1952). "Fluid flow through packed columns." *Chem. Eng. Proc.*, 48, 1159-1184.

26- Wen, C. Y. and Yu, H. (1966). Mechanics of fluidization. Chem Engng Prog. Symp. Ser., 62, 100-111.

27- Gidaspow, D. (1994). Multiphase Flow and Fluidization: Continuum and Kinetic Theory Description. *Academic Press, New York.*

28- Xu, G. and Kato, K. (1999). "Hydrodynamic equivalent diameter for clusters in heterogeneous gas–solid flow." *Chem. Eng. Sci.*, 54, 1837–1847.

29- Bi, H. T. (2002). "Some issues on core-annulus and cluster models of circulating fluidized bed reactors." *Can. J. Chem. Eng.*, 80, 809–817.

30- Harris, A. T., Davidson, J. F. and Thorpe, R. B. (2002). The prediction of particle cluster properties in the near wall region of a vertical riser. Powder Technol., 127, 128–143.

31- Mostoufi, N. and Chaouki, J. (2004). "Flow structure of the solids in gas- solid Fluidized beds." *Chem. Eng. Sci.*, 54, 4217- 4227.

32- Mostoufi, N. and Chaouki, J. (2000). "On the axial movement of solids in gas–solid fluidized beds." *Trans. Inst. Chem. Eng.*, 78, 911–920.

33- Zuber, N. (1964). "On the dispersed two-phase flow in the laminar flow regime." *Chem. Eng. Sci.*, 19, 897–917.

34- Gu, W. K. and Chen, J. C. (1998). A model for solid concentration in circulating fluidized beds. In: Fan, L.S., Knowlton, T.M. (Eds.), Fluidization IX. Engineering Foundation, Durago, Colorado. 501–508.

35- Zou, B., Li, H., Xia, Y. and Ma, X. (1994). Cluster structure in a circulating fluidized bed. Powder Technol., 78, 173–178.